The Effect of Structural Parameters on the Electronic States and Oscillator Strength of a Resonant Tunneling Quantum Well Infrared Photodetector

Reza Masoudian Saadabad and Naser Hatefi-Kargan*

Department of Physics, University of Sistan and Baluchestan, Zahedan, Iran

***Corresponding Author Email:** n.hatefi@phys.usb.ac.ir

ABSTRACT— In this paper a resonant tunnelling quantum well infrared photodetector (RT-QWIP) is discussed. Each period of this photodetector structure comprises of a resonant tunnelling structure (AlAs/AlGaAs/AlAs) nearby a quantum well (AlGaAs/GaAs). In this photodetector, photocurrent is produced when an electron makes a transition from the ground state of the well to an excited state which is coupled to the resonant state of the resonant tunnelling structure. The effect of structural parameters of the photodetector on the electronic states and oscillator strength of transitions between energy subbands of the structure is investigated. Then using the obtained results, an appropriate structure for the RT-QWIP is determined which exhibits a photoresponse peak at 7.3 μm at 77 K.

KEYWORDS: Infrared, Oscillator Strength, Photodetector, Quantum Well.

I. INTRODUCTION

The increasing interest in the infrared region of the electromagnetic spectrum is due to its numerous applications such as navigation, warning systems, and imaging [1]. To develop better devices and tools for these applications, it is required to design and build infrared detectors to operate at high temperatures. Generally, infrared photodetectors need low dark current and this is usually achieved using a cooling system associated with the photodetectors. One of the most widely used techniques for infrared detection is using intersubband absorption in quantum wells [2], and GaAs based quantum well photodetectors have been widely studied and used [2-6]. As stated earlier, to use these photodetectors a cooling system is required to reduce the dark current originating from the thermal excitations. However, the use of a cooling system has significant impacts on the cost and dimensions of the infrared detectors. To avoid these problems, one can use a resonant tunnelling Double Barrier Structure (DBS) as a current filter in the design of a Quantum Well Infrared Photodetector (QWIP). This composite structure is termed Resonant Tunnelling Quantum Well Infrared Photodetector (RT-QWIP). Initially, a few designs of quantum dot infrared photodetectors were proposed in which a resonant tunnelling double barrier structure was used for each quantum dot layer and it was observed that such quantum dot infrared photodetectors are working well at room temperature (300 K) [7,8]. Later, a multi-band tunnelling quantum dot infrared photodetector was proposed covering the range from mid- to far-infrared in which two resonant tunnelling double barrier structures are attached on both sides of quantum dot layers [9]. Moreover, the use of resonant tunnelling barriers was reported in terahertz quantum dot infrared photodetectors [8] and more recently in quantum ring photodetectors [10]. Brave *et al*. [11] showed that resonant tunnelling barriers significantly decreased the dark current density and increased the specific detectivity in a quantum dots-in-a-well infrared photodetector. Although the studies mentioned above have investigated the effect of resonant

tunnelling on quantum dots, a limited number of studies have investigated the effect of resonant tunnelling in quantum wells. Zhu *et al.* [12] showed that using a resonant tunnelling double barrier heterostructure in a strained-layer superlattice infrared photodetector has significantly suppressed the dark current. In order to optimize the design of a RT-QWIP, we need to have a comprehensive knowledge of the parameters influencing the intersubband absorption, photocurrent, and dark current. The objective of this study is to analyse the effect of the structural parameters on the electronic states and intersubband oscillator strength of a RT-QWIP.

In this paper, the design of a RT-QWIP is theoretically studied where a resonant tunnelling double barrier structure is incorporated to each quantum well layer. The ground energy level of each period is located inside the quantum well of the period and the excited energy levels are outside the quantum well. The ground state electrons in the well can absorb infrared photons from an incident radiation to provide enough energy for transitions to excited states. A particular excited state is coupled with a resonant state of the DBS. Electron transition from the ground state to this excited state gives the peak value of the oscillator strength curve. The electrons made transitions to this particular energy state can tunnel through the DBS and generate photocurrent in the RT-QWIP while the DBS blocks other electrons from passing through the structure. In other words, the DBS acts as a filter which separates the photocurrent from the dark current by blocking the electrons contributing in the dark current.

In the present study, first effect of the distance of the quantum well from the DBS on the electronic states and intersubband oscillator strength of the structure is investigated. Then, the effect of the width of the barriers of the DBS and the distance between the barriers of the DBS on the mentioned parameters are studied. Finally, by using the obtained results an optimum structure for the RT-QWIP is determined. Each period of the structure considered in this study comprises of an $AlAs/Al_{0.2}Ga_{0.8}As/AlAs$ DBS, and an $Al_{0.2}Ga_{0.8}As/GaAs$ quantum well.

II. Geometry and Mathematics

In this paper, a RT-QWIP is designed and the effects of structural parameters on its performance are studied. Each period of the photodetector comprises of an $AlAs/Al_{0.2}Ga_{0.8}As/AlAs$ resonant tunnelling double barrier structure adjacent to a 40 Å GaAs well. The width of the well is considered 40 Å so that the ground energy level of the well becomes a bound state but excited energy levels make the continuum states. The conduction band edge structure of the RT-QWIP under zero bias is schematically shown in Fig. 1. The growth direction of the structure is considered along [100] direction of the crystal, which is considered as z axis. The figure shows the optimum situation in which the excited state of the quantum well is coupled to the resonant state of the DBS. The structural parameters are width of the quantum well, width of the barriers of the DBS, distance between the barriers of DBS, and the distance of the quantum well from the DBS. These parameters are indicated by L_W, L_B, L_{BB}, and L_{WB} in Fig. 1, respectively.

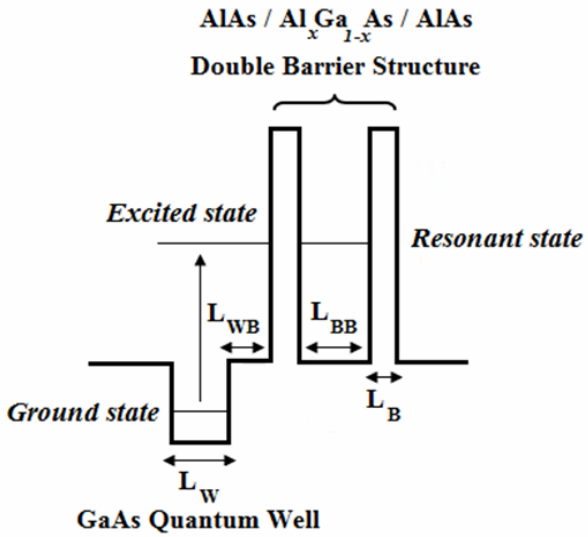

Fig. 1. Conduction band edge structure of an optimum RT-QWIP under zero bias. The excited state of the quantum well is coupled with the resonant state of the DBS.

There are several well-known models for calculating electronic energy and wavefunctions of semiconductor quantum well structures. In this paper, the single band effective mass model was used. Although the single band effective mass model does not work well for valance band electrons, it works well for conduction band electrons [13], which is the purpose of this study. For a semiconductor heterostructure, the single band effective mass equation is given by,

$$\left[-\frac{\hbar^2}{2m^*(z)}\frac{\partial^2}{\partial z^2}+V(z)\right]\psi(z)=E\psi(z) \tag{1}$$

where $\hbar$ is the reduced Plank constant, $\psi(z)$ is the envelope function of the electron wavefunction, E is the energy eigenvalue associated with the envelope function, and $m^*(z)$ is the effective mass. The $V(z)$ is the potential energy discontinuity in the conduction band edge and can be represented by,

$$V(z)=0.6\left[E_g^{Barrier}-E_g^{Well}\right] \tag{2}$$

where E_g is the energy gap at the Γ point [14]. All through this paper top of the well in Fig. 1 is considered as zero energy level. Electron wavefunction, $\phi(\mathrm{r})$, is represented by,

$$\varphi(\mathbf{r})=u_\upsilon(\mathbf{r})\,f(\mathbf{r});\qquad f(\mathbf{r})=\frac{1}{\sqrt{s}}\exp\left(i\,\mathbf{k}_\perp\cdot\mathbf{r}_\perp\right)\,\psi(z) \tag{3}$$

where $u_\upsilon(\mathbf{r})$ is the periodic part of the Bloch function, $\mathbf{k}_\perp$ and $\mathbf{r}_\perp$ are the two dimensional wave and position vectors in the plane of the quantum well layers, and $\psi(z)$ is the envelope wavefunction. The effective mass is as a function of the growth direction of the heterostructure, z, and the two dimensional wave number but the effect of the latter is usually ignored in the single band model [13]. Note that the kinetic energy operator in Eq. 1 is not Hermitian, in order to have a Hermitian operator Eq. 1 should be rewritten as follow,

$$-\frac{\hbar^2}{2}\frac{\partial}{\partial z}\frac{\partial\psi(z)}{m^*(z)\partial z}+V(z)\psi(z)=E\psi(z) \tag{4}$$

The effect of an electric field along the growth axis, *F*, on the energy levels is approximated by the second order perturbation theory [15] as follows,

$$\Delta E^{(2)}=\sum_{f\rangle i}^{\infty}\left|\langle\psi_f|-eFz|\psi_i\rangle\right|^2\frac{1}{E_f-E_i} \tag{5}$$

where *e* is the electric charge and subscripts *i* and *f* represent the initial and final states in the electron transition, respectively. In order to investigate the effect of an incident electromagnetic radiation on the behaviour of the heterostructure, a linearly polarized planar electromagnetic wave has been considered with an electric field as follows,

$$\mathbf{F}=F_0\boldsymbol{\varepsilon}\cos(\omega t-\mathbf{k}\cdot\mathbf{r}) \tag{6}$$

where $\boldsymbol{\varepsilon}$ is the polarization, ω is the angular frequency, and $\mathbf{k}$ is the wave vector along the propagation direction of the electromagnetic wave. If the heterostructure is exposed to this electromagnetic wave, the transition rate from the initial state to final state is given by Fermi's golden rule [16],

$$\frac{1}{\tau_i}=\frac{2\pi}{\hbar}\sum_f\left|\langle\psi_f(r)|\tilde{\mathrm{H}}|\psi_i(r)\rangle\right|^2\times\delta(E_f-E_i\pm\hbar\omega) \tag{7}$$

where $\tilde{\mathrm{H}}$ is the time-dependent perturbation Hamiltonian due to electromagnetic field, and δ is the Kronecker delta function. Note that the sign of the photon energy term is positive for emission and negative for absorption. The heterostructure can act as a two-dimensional micorcavity and hence the intersubband transition rate can be rewritten as follows [15],

$$\frac{1}{\tau_i}=\frac{e^2\omega}{4\varepsilon\, m^*c^2L_w}O_{if} \tag{8}$$

where ε is the permittivity, and *c* is the speed of light. The dimensionless quantity O_{if}, is the oscillator strength and is dependent upon the dipole matrix element [15],

$$O_{if}=\frac{2m^*\omega}{\hbar}\left|\langle\psi_i|z|\psi_f\rangle\right|^2 \tag{9}$$

In this study, the transmission probability of the electron through the DBS, $T(E_z)$, was determined using the transfer matrix method [14].

III. RESULT AND DISCUSSION

At first, in order to assess the validity of the simulations, intersubband absorption in a multiple quantum well (MQW) was considered. It consisted of 70 periods of 75 Å undoped GaAs quantum wells and 100 Å barriers of silicon doped $Al_{0.3}Ga_{0.7}As$ ($n = 1\times10^{18}$ cm^{-3}). The intersubband absorption can be calculated by [17],

$$\alpha(\upsilon) = \left(\frac{\pi\, e^2\hbar\, O_{if}}{2\varepsilon_0 m^* c\, n_r}\right)\frac{\left(n_i - n_f\right)\cos^2(\theta)\;\; \gamma/2\pi}{\left(E_f - E_i - h\upsilon\right)^2 + \left(\gamma/2\right)^2} \quad (10)$$

where υ is the optical frequency of the incident electromagnetic wave, h is the Plank constant, n_i and n_f are three-dimensional density of carriers in initial and final state subbands, respectively. γ is the full width at half maximum of the absorption lineshape, θ is the angle between the z direction and the electric field of the electromagnetic wave incident on the photodetector, n_r is the index of refraction, and ε_0 is the permittivity in vacuum. For evaluation of our computer codes, we assumed $\theta = 60^o$ in order to be able to compare our results with the results in [18], and the inverse of electromagnetic wavelength at peak position of the intersubband absorption, denoted as k_p, was calculated as a function of temperature, Fig. 2. In this calculation, effective mass of electrons in the wells was considered as a function of temperature, using the same temperature dependence as in [18], and then by solving the effective mass equation energy levels and wavefunctions were calculated. Then by using Eq. 10 absorption spectra were calculated and the k_p at peak absorption points were obtained. There is a gradual increase in the value of the k_p with the increase of temperature. This increase is more significant between 100 K and 300 K so that the value of the k_p increases from 960 cm^{-1} in 100 K to about 978 cm^{-1} in 300 K. As shown in the figure, these results are in good agreement with those reported by Szmulowicz *et al*. [18]. This indicates that our computer codes works well.

In order to investigate the effect of the structural parameters on the electronics states and oscillator strength, three different RT-QWIPs were devised. In each case, the effect of one of the structural parameters has been studied. For this purpose, each structural parameter varied from a minimum to a maximum value by 2 Å steps while other parameters were constant.

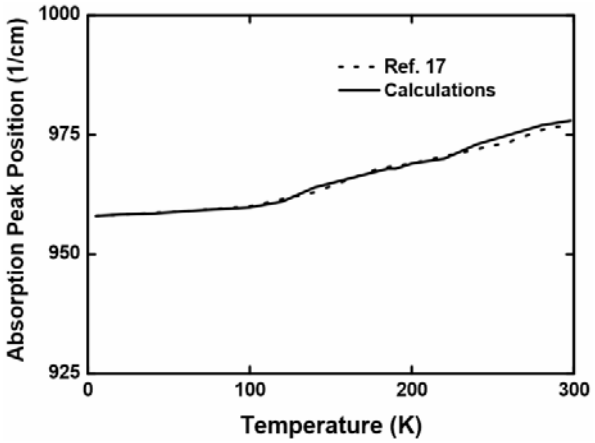

Fig. 2. The peak position of intersubband absorption, k_p, in the MQW as a function of temperature. Calculations (solid line) are in good agreement with those reported by Szmulowicz *et al.* [18].

The structural parameters for the first case are given in Table 1 where L_{WB} varies from 10 to 60 Å while L_B and L_{BB} are fixed at 20 and 40 Å, respectively. The energy eigenvalue associated with the peak position of oscillator strength (E_p), i.e. the excited state as shown in Fig. 1, has been shown in Fig. 3. E_p shows staircase-shaped behavior with the increase of L_{WB}, E_p decreases slightly at each step of the staircase-shaped curve while there is a sharp drop at the end of each one. The sharp drop is due to the substitution of excited state with a lower one. We also found a relatively linear relationship between the peak value of oscillator strength and L_{WB}, Fig. 4. The wavefunction associated with the peak position of oscillator strength is more localized in the well region for large values of L_{WB} in comparison with the small values of L_{WB}. Consequently, wavefunction overlap between the excited state and the ground state increases as the value of the L_{WB} increases. Therefore this leads to the increase of the oscillator strength at peak point.

Table 1. The structural parameters considered for studying the effect of L_{WB} on the electronic states and the oscillator strength of RT-QWIP.

Parameter	Type	Value	Unit
L_W	Constant	40	Å
L_B	Constant	20	Å
L_{BB}	Constant	40	Å
L_{WB}	Variable	10 - 60	Å

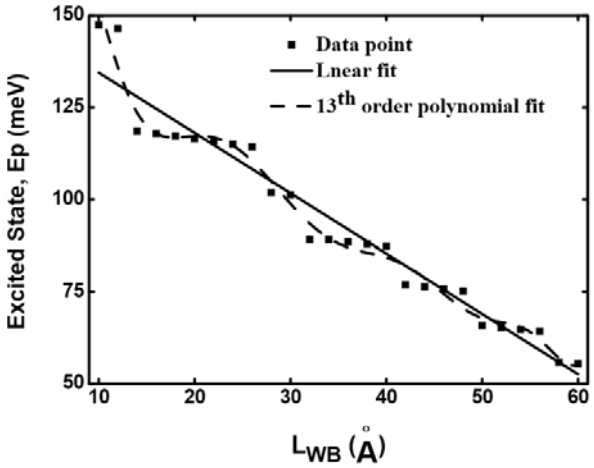

Fig. 3. Staircase-shaped behaviour of E_p as a function of L_{WB}. L_{WB} varies from 10 to 60 Å while L_B and L_{BB} are fixed at 20 and 40 Å, respectively. The calculated E_p is illustrated by solid squares and its linear fit and 13th order polynomial fit is illustrated by solid line and dashed line, respectively.

Table 2. The structural parameters considered for studying the effect of L_{BB} on the electronic states and the oscillator strength of RT-QWIP.

Parameter	Type	Value	Unite
L_W	Constant	40	Å
L_B	Constant	20	Å
L_{BB}	Variable	10-60	Å
L_{WB}	Constant	10	Å

In the second case, the parameter L_{BB} varied from 10 to 60 Å while parameters L_{WB} and L_B were fixed at 10 and 20 Å, respectively, as given in Table 2. Fig. 5 shows that E_p increases as the value of L_{BB} decreases. In contrast with the first case there is no staircase-shaped behaviour for E_p since the excited state never substituted by another excited state. Therefore, E_p shows a linear downward trend when the distance between the barriers of DBS, L_{BB}, increases. In addition, the peak value of oscillator strength shows a similar behaviour when L_{BB} becomes thicker, Fig. 6.

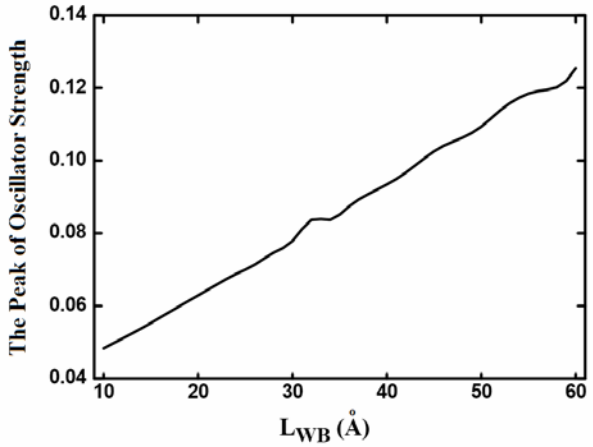

Fig. 4. A linear relationship between the peak value of oscillator strength and L_{WB}. The parameter L_{WB} varies from 10 to 60 Å, while the parameters L_B and L_{BB} are fixed at 20 and 40 Å, respectively.

However, it can be seen that the drop in the peak value of oscillator strength is negligible (less than 0.002). The relationship between the resonant energy level of DBS, E_R, and L_{BB} was also investigated and the results are shown in Fig. 7. It can be seen that when L_{BB} increases from 10 Å to 60 Å the value of E_R dramatically decrease to 80 meV from 500 meV.

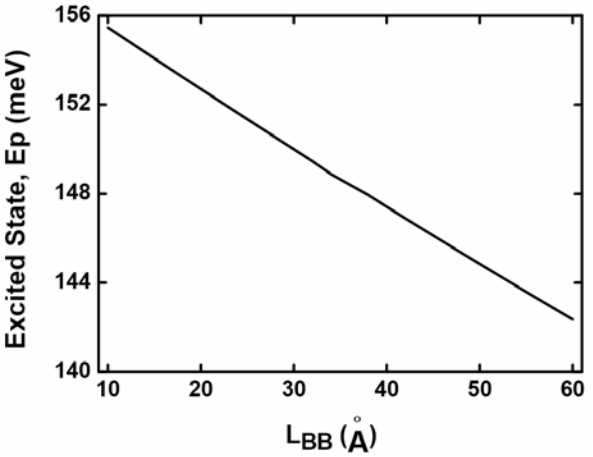

Fig. 5. E_p increases as the value of L_{BB} decreases. The parameter L_{BB} varies from 10 to 60 Å while parameters L_{WB} and L_B were fixed at 10 and 20 Å, respectively.

In the third case, effect of the width of the barriers of the DBS, L_B, on the oscillator strength and the electronic states were

investigated. For this purpose, the parameters L_{WB} and L_{BB} were fixed at 10 and 40 Å, respectively while parameter L_B varied from 10 to 50 Å, as listed in Table 3.

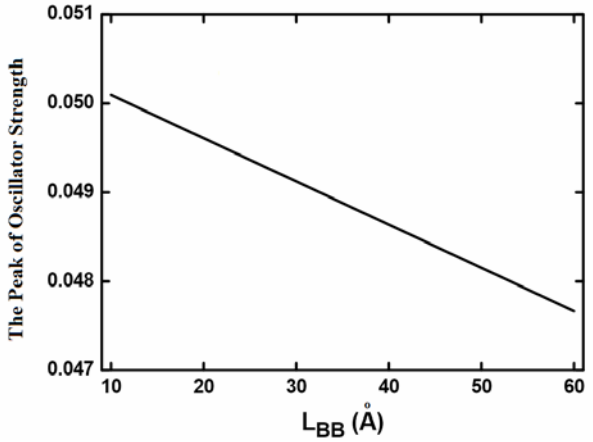

Fig. 6. The peak value of the oscillator strength as a function of L_{BB}. The parameter L_{BB} varies from 10 to 60 Å while parameters L_{WB} and L_B are fixed at 10 and 20 Å, respectively. It can be seen that the drop in the peak value of the oscillator strength is negligible (less than 0.002).

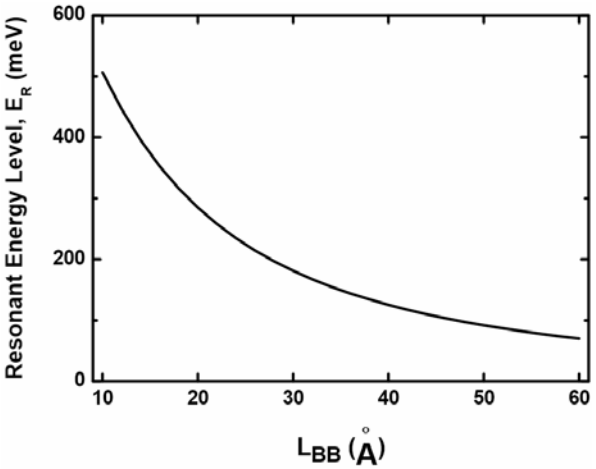

Fig. 7. The relationship between the resonant energy level of DBS, E_R, and the distance between the barriers of DBS, L_{BB}. Parameters L_{WB} and L_B are fixed at 10 and 20 Å, respectively, but L_{BB} varies from 10 to 60 Å.

As illustrated in Fig. 8, continuous increase in L_B leads to staircase-shaped behaviour for E_p. Increasing L_B results in the reduction of the interactions between the resonant states localised within the DBS and the excited state of the quantum well. This reduction in interactions leads to a small decrease in the energy levels of the well which results in the decrease of E_p at higher values of L_B.

Table 3. The structural parameters considered for studying the effect of L_B on the electronic states and the oscillator strength of RT-QWIP.

Parameter	Type	Value	Unite
L_W	Constant	40	Å
L_B	Variable	10 - 50	Å
L_{BB}	Constant	40	Å
L_{WB}	Constant	10	Å

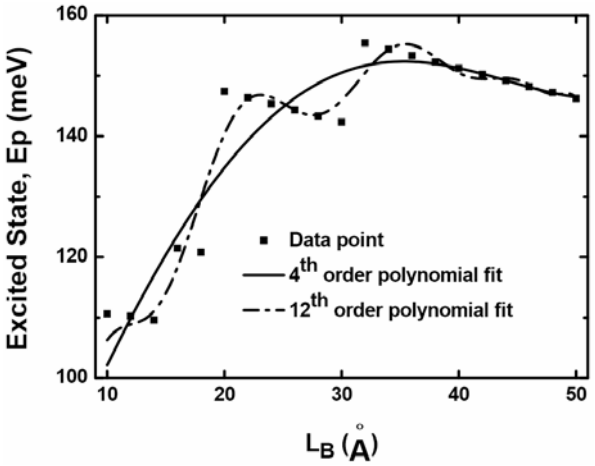

Fig. 8. Continuous increase in L_B leads to staircase-shaped behaviour for E_p. The parameters L_{WB} and L_{BB} are fixed at 10 and 40 Å, respectively, while parameter L_B varies from 10 to 50 Å.

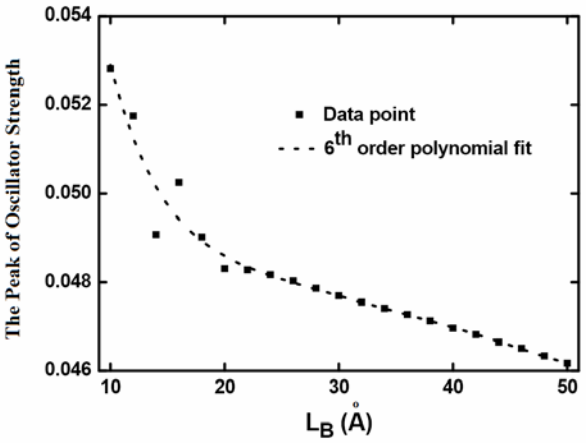

Fig. 9. The peak value of oscillator strength as a function of L_B. Apart from the fluctuations, it can be concluded that the peak value of oscillator strength decreases as L_B increases (6th order polynomial fit). L_{WB} and L_{BB} are fixed at 10 and 40 Å, respectively, while parameter L_B varies from 10 to 50 Å.

As the 4th order polynomial fit shows, E_p dramatically rises from above 100 meV at L_B=10 Å to over 150 meV at L_B=35 Å. Fig. 9 shows the peak value of oscillator strength as a function of L_B, it can be seen that the peak value of oscillator strength fluctuates between

0.053 and 0.048 when L_B varies from 10 Å to 20 Å. When the value of L_B is higher than 20 Å, the peak value of oscillator strength decreases slightly. Apart from the fluctuations, it can be concluded that the peak value of oscillator strength decreases as L_B increases (6^{th} order polynomial fit). Finally, the effect of L_B on the parameter E_R was investigated and the results are illustrated in Fig. 10. The resonance energy increases with increasing the width of the barriers of the DBS due to confinement effects. When L_B varies from 10 Å to 16 Å, E_R increases from about 123 meV to about 125 meV, and thereafter E_R flattens off and no longer changes as L_B increases.

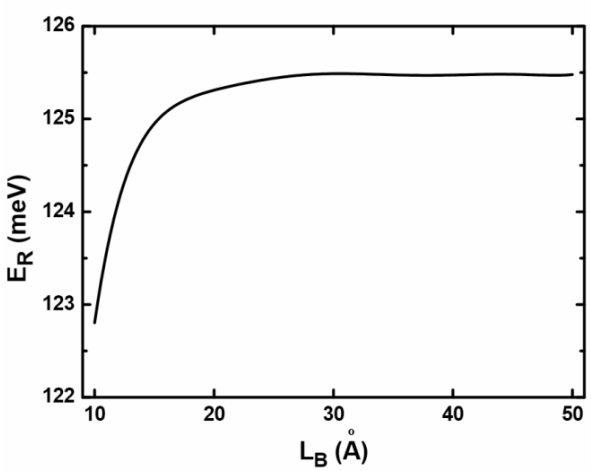

Fig. 10. The resonance energy increases with increasing the width of the barriers of DBS, L_B. The major changes occurs when L_B is in the range of 10 -16 Å. The parameters L_{WB} and L_{BB} were fixed at 10 and 40 Å, respectively while parameter L_B varied from 10 to 50 Å.

The obtained results have been used to determine an optimum structure for the RT-QWIP in which the excited state is coupled to the resonant state. The structural parameters have to be selected so that the values of E_p and E_R are equal. As illustrated in Fig. 6, variation in the value of L_{BB} does not significantly change the peak value of oscillator strength and hence it can be considered that the peak value of oscillator strength does not depend on L_{BB}. As shown in Fig. 7, we can find a low value for E_R as long as the value of L_{BB} is large. The L_{BB} was chosen to be 47 Å since additional increase in its value does not significantly change E_R. Moreover, a very large L_{BB} cannot be chosen since electrons may be scattered before passing through the DBS. In liquid nitrogen temperature, 77 K, energy uncertainty for an excited state is about 20 meV (i.e. $\Delta E = 20$ meV) [17]. Therefore, by using Heisenberg's momentum-space uncertainty principle and the effective mass of electrons, mean free path of an electron that has a z component energy between 95 – 105 meV relative to the top of quantum well is between 116 – 122 Å. Hence, the sum of L_{WB} + L_{BB} + $2L_B$ must be less than 116 – 122 Å to avoid electron scattering before passing through the DBS. For this reason, L_{WB} and L_B have been chosen to be 22 and 12 Å, respectively. We have deliberately chosen a large value for L_{WB} and a small value for L_B, since such values can lead to the large peak value of oscillator strength (see Fig. 4 and Fig. 9). With these choices, E_p and E_R became 97 and 99 meV, respectively. A 2 meV difference in energy between E_p and E_R is very small and can be neglected. This means that the peak state has been coupled to the resonant state of the DBS, i.e. RT-QWIP has been optimized. The structural parameters for the optimum RT-QWIP are listed in Table 4. The normalized oscillator strength of the optimum RT-QWIP is also illustrated in Fig. 11(a). It can be seen that the peak position of the oscillator strength, i.e. the operating wavelength of the RT-QWIP, is located at 7.3 μm. In addition, the wavefunctions associated with the ground state and the excited states have been illustrated in Fig. 11(b). As the figure shows, the amplitude of peak state is significantly large within the region of the DBS. This large amplitude is an evidence of resonant tunnelling through the DBS. The transmission coefficient of DBS at zero bias has been shown in Fig. 11(c) where it can be seen that the first resonant energy occurs at 99 meV. In order to calculate the transmission coefficient transfer matrix method was used as has been explained in [19]. It should be also mentioned that the application of electric fields in the range from 0 to 2×10^6 V/m on the RT-QWIP did not influence E_p, but E_R linearly decreased to 88 meV. Typical QWIPs generally operate under electric fields lower than 1×10^6 V/m. Therefore, applying electric field on the

optimum RT-QWIP leads to a 3-4 meV difference in energy between E_p and E_R that can be neglected. Nevertheless, this difference could be decreased with slight reduction of L_{BB}.

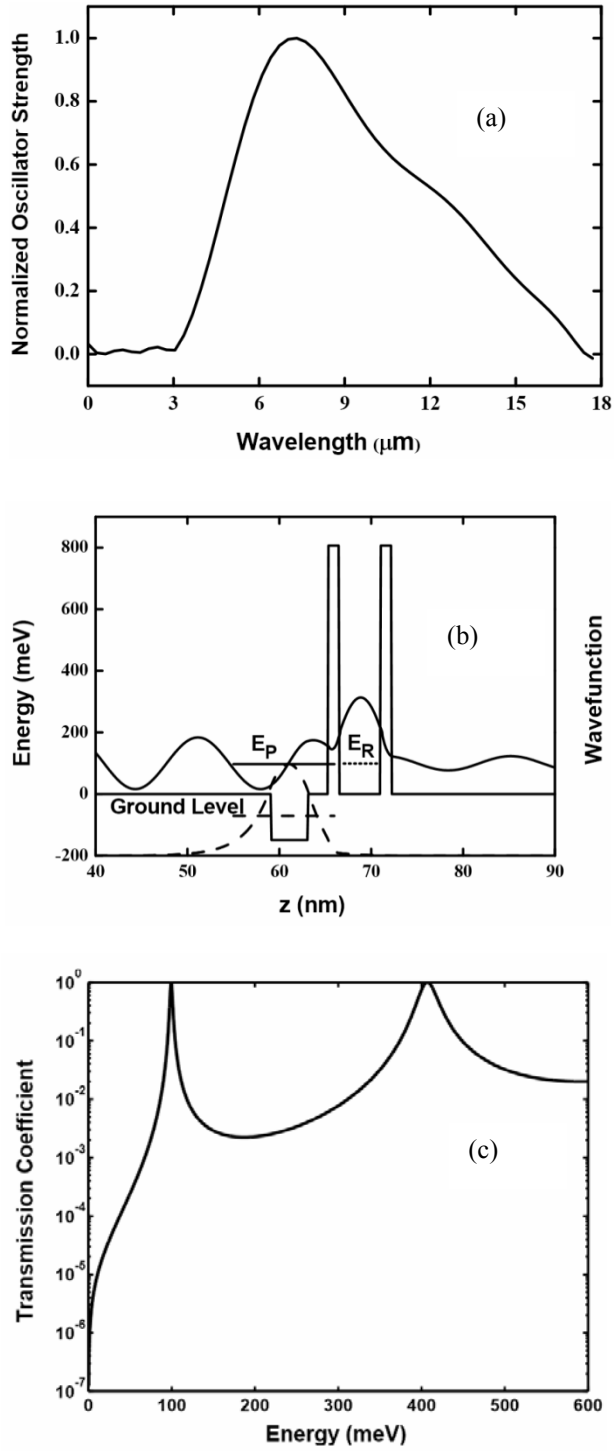

Fig. 11. (a) The normalized oscillator strength of the optimum RT-QWIP (b) The wavefunction associated with the ground state and the peak state are illustrated by dashed and solid lines, respectively. The large amplitude of the excited state within the region of DBS is an evidence of resonant tunnelling through the DBS. (c) The transmission coefficient for DBS at zero bias. The first resonant energy occurs at 99 meV.

Table 4. The structural parameters for the optimum RT-QWIP are listed.

L_W	L_{WB}	L_B	L_{BB}
40 Å	22 Å	12 Å	47 Å

IV. CONCLUSION

We discussed the characteristics of a RT-QWIP consisting of a DBS near a quantum well. The effects of structural parameters of the RT-QWIP on the electronic states and oscillator strength were analysed. Using the obtained results, an optimum structure for the RT-QWIP was determined in which the excited state energy level has been coupled to the resonant energy level of the DBS. The operation wavelength of the optimum RT-QWIP is 7.3 μm at 77 K.

REFERENCES

[1] A. Rogalski, *Infrared Detectors*, Boca Raton: CRC Press, 2011.

[2] T. Miyatake, S. Horihata, T. Ezaki, H. Kubo, N. Mori, K. Taniguchi, and C. Hamaguchi, "GaAs/AlGaAs quantum well infrared photodetectors," Solid State Electron. Vol. 37, pp. 1187–1190, 1994.

[3] W. Liu, D.H. Zhang, Z.M. Huang, and W.J. Fan, "Theoretical study of quantum well infrared photodetectors with asymmetric well and barrier structures for broadband photodetection," J. Appl. Phys. Vol. 101, pp. 033114 (1-7), 2007.

[4] G. Hasnain, B.F. Levine, C.G. Bethea, R.A. Logan, J. Walker, and R.J. Malik, "GaAs/AlGaAs multiquantum well infrared detector arrays using etched gratings," Appl. Phys. Lett. Vol. 54, pp. 2515-2517, 1989.

[5] B.F. Levine, S.D. Gunapala, J.M. Kuo, S.S. Pei, and S. Hui, "Normal incidence hole intersubband absorption long wavelength $GaAs/Al_xGa_{1-x}As$ quantum well infrared photodetectors," Appl. Phys. Lett. Vol. 59, pp. 1864-1866, 1991.

[6] B.K. Janousek, M.J. Daugherty, W.L. Bloss, M.L. Rosenbluth, M.J. O'Loughlin, H. Kanter, F.J. De Luccia, and L.E. Perry,

‘‘High-detectivity GaAs quantum well infrared detectors with peak responsivity at 8.2 μm,” J. Appl. Phys. Vol. 67, pp. 7608-7611, 1990.

[7] X. Su, S. Chakrabarti, P. Bhattacharya, G. Ariyawansa, and A.G.U. Perera, “A resonant tunnelling quantum-dot infrared photodetector,” IEEE J. Quantum Electron. Vol. 41, pp. 974-979, 2005.

[8] P. Bhattacharya, X.H. Su, S. Chakrabarti, G. Ariyawansa, and A.G.U. Perera, “Characteristics of a tunnelling quantum-dot infrared photodetector operating at room temperature,” Appl. Phys. Lett. Vol. 86, pp. 191106 (1-3), 2005.

[9] A.G.U. Perera, G. Ariyawansa, V.M. Apalkov, S.G. Matsik, X.H. Su, S. Chakrabarti, and P. Bhattacharya, “Wavelength and polarization selective multi-band tunnelling quantum dot detectors,” Opto-Electron. Rev. Vol. 15, pp. 223–228, 2007.

[10] G. Huang, W. Guo, P. Bhattacharya, G. Ariyawansa, and A.G.U. Perera, “A quantum ring terahertz detector with resonant tunnel barriers,” Appl. Phys. Lett. Vol. 94, pp. 101115 (1-3), 2009.

[11] A. Barve, S. Member, J. Shao, Y.D. Sharma, S. Member, T.E. Vandervelde, K. Sankalp, S.J. Lee, S.K. Noh, and S. Krishna, “Resonant tunnelling barriers in quantum dots-in-a-well infrared photodetectors,” IEEE J. Quantum Electron. Vol. 46, pp. 1105–1114, 2010.

[12] Z.M. Zhu, P. Bhattacharya, E. Plis, X.H. Su, and S. Krishna, “Low dark current InAs/GaSb type-II superlattice infrared photodetectors with resonant tunnelling filters,” J. Phys. D: Appl. Phys. Vol. 39, pp. 4997–5001, 2006.

[13] B.R. Nag, *Physics of Quantum Well Devices*, Dordrecht: Kluwer Academic Publishers, 2000.

[14] H. Mizuta and T. Tanoue, *The Physics and Applications of Resonant Tunnelling Diodes*, New York: Cambridge University Press, 1995.

[15] P. Harrison, *Quantum Wells, Wires and Dots: Theoretical and Computational Physics of Semiconductor Nanostructure*, New York: John Wiley & Sons, 2005.

[16] R. Paiella, *Intersubband Transitions in Quantum Structures*, New York: McGraw-Hill, 2006.

[17] S.L. Chuang, *Physics of Photonic Devices*, New Jersey: John Wiley & Sons, 2009.

[18] F. Szmulowicz, M.O. Manasreh, D.W. Fischer, F. Madarasz, K.R. Evans, E. Stutz, and T. Vaughan, “The temperature dependence of intersubband absorption in a barrier-doped $GaAs/Al_{0.3}Ga_{0.7}As$ quantum well structure,” Superlattice. Microst. Vol. 8, pp. 63-67, 1990.

[19] H. Mizuta, T. Tanoue, and A. Rogalski, *The Physics and Applications of Resonant Tunnelling Diodes*, New York: Cambridge University Press, 2006.

Reza Masoudian Saadabad received his M.Sc. degree in Solid State Physics from the University of Sistan and Baluchestan in February 2011. He did his M.Sc. thesis on "Desiging a Quantum Well Infrared Photodetector Containing a Current Filter". His research interest is theoretical modeling of quantum well devices.

Naser Hatefi-Kargan recievied his PhD degree from the University of Leeds in June 2007. He is now with the Physics Department of the University of Sistan and Baluchestan as an assistant professor. Dr. Hatefi-Kargan is a member of both Optics and Photonics Society and the Physics Society of Iran. His research areas are semiconductor photonic devices and plasmonic sensors.

THIS PAGE IS INTENTIONALLY LEFT BLANK.